Available online at www.sciencedirect.com
SCIENCE DIRECT®
Journal of Power Sources 129 (2004) 303–311
JOURNAL OF POWER SOURCES
www.elsevier.com/locate/jpowsour

In situ preparation of poly(ethylene oxide)–SiO_2 composite polymer electrolytes

Y. Liu, J.Y. Lee*, L. Hong

Department of Chemical and Environmental Engineering, National University of Singapore, 10 Kent Ridge Crescent, Singapore 119260, Singapore

Received 11 August 2003; accepted 10 November 2003

Abstract

Amorphous poly(ethylene oxide) (PEO)–SiO_2 composites are prepared by in situ reactions that involve the simultaneous formation of the polymer network and inorganic nanoparticles. The polymer matrix is formed by ultraviolet irradiation of a PEO macromer, and silica is produced in situ by the sol–gel method. The PEO–SiO_2 composite mixed with $LiBF_4$ is used as a lithium-ion conducting solid electrolyte and electrochemical transport properties such as ionic conductivity and Li^+ transference number are measured. A significant increase in the Li^+ transference number, up to 0.56, is found together with a slight decrease in the ionic conductivity. The results are interpreted in terms of interactions between the surface OH groups of the inorganic particles, the cations, the anions, and the ether oxygen atoms on the PEO backbone.

Keywords: Nanocomposite; Lithium battery; Sol–gel; Ultraviolet irradiation; Poly(ethylene oxide); Solid polymer electrolyte

1. Introduction

Among the many applications proposed for solid polymer electrolytes [1–3], their deployment in lithium-based secondary batteries has the greatest impact in terms of technology and market potential. Compared with their liquid counterparts, polymer electrolytes have the advantage of longer shelf-life, leak-proof construction, and easy fabrication into a wide variety of shapes and sizes [4]. Conventional polymer electrolytes are constituted from a high molecular weight polymer, e.g., poly(ethylene oxide) (PEO) and a lithium salt, e.g., $LiCF_3SO_3$. It is widely accepted that PEO can complex with a large number of lithium salts, and that the Li^+ conductivity is strongly dependent on the segmental motion of the polymer backbone. Thus, significant ion conduction only occurs in the amorphous phase, where the conductivity is two to three orders of magnitude higher than in the crystalline region [5]. Nevertheless, the polymer electrolyte system as a whole still suffers from low ionic conductivity ($\sigma < 10^{-7}\,S\,cm^{-1}$ at room temperature) because of the partial crystallinity of the polymer component.

Most approaches to increase the ionic conductivity of PEO systems are based on lowering the degree of PEO crystallization or reducing the glass transition temperature. A variety of methods may be used, e.g., polymer structure modifications [6,7], and the incorporation of plasticizers [8,9] or ceramic fillers [10,11]. The highest conductivity reported to date is close to that of liquid electrolytes ($\sim 10^{-3}\,S\,cm^{-1}$ at room temperature) and is achieved in gel polymer electrolytes (GPE). The latter are prepared by immobilizing a high concentration of low molecular weight plasticizers in a polymer network. Such construction, however, compromises dimensional stability and GPE cannot be used in a battery without a separator. While immobilized, liquid components remain present in the GPE construction and this raises concerns about safety and reliability in applications.

A good approach to an all solid-state design through the addition of ceramic fillers has been proposed by Weston and Steele [10]. Their pioneering work was followed by comprehensive studies of the properties of polymer composites, such as conductivity [12], crystallinity [13] and thermal behaviour [14]. It generally observed that both the ionic conductivity and the mechanical properties are improved after the addition of ceramic fillers, and the properties of the composite electrolytes are dependent on particle size [15], concentration and surface chemistry [16,17]. The conductivity enhancement is commonly attributed to a decrease in polymer crystallinity, and an enlargement of the amorphous domains in the PEO matrix. Recently, it has been concluded [18,19] that Lewis acid–base type interactions between ceramic fillers contribute to the increase in conductivity.

* Corresponding author. Tel.: +65-6874-2899; fax: +65-6779-1936.
E-mail address: cheleejy@nus.edu.sg (J.Y. Lee).

0378-7753/$ – see front matter © 2003 Elsevier B.V. All rights reserved.
doi:10.1016/j.jpowsour.2003.11.026

In most of the reported work, the polymer component is crystalline PEO. The addition of ceramic particles is unable to suppress polymer crystallization completely, and results in a multiphase structure (simultaneous presence of both crystalline and amorphous phases) for the polymer composites. This causes considerable complications in interpreting the influence of ceramic fillers. Amorphous PEO [20–22] has been used to identify the effects of ceramic particles other than as disruptors of polymer crystallinity. This procedure has been used for the preparation of composite membranes. The increase in conductivity can be rationalized in terms of mobility enhancements of the polymer segments and the salt after the nanoparticle addition.

The particle size of the ceramic filler is a key factor in determining the properties of composite polymer electrolytes, with smaller particle size providing the most pronounced effects. Hence, a substantial amount of work has been devoted to the use of nanoscale ceramic particles, such as γ-$LiAlO_2$ [12], Al_2O_3 [15], and SiO_2 [23]. The polymer composites in these studies were made by mechanical blending, in which the aggregation of nanoparticles is an inevitable event due to the high surface energy of small particles. The end result is limited efficacy of the ceramic fillers. A simple and effective method to address this problem was reported recently [24–26]. This used sol–gel chemistry to precipitate nanoscale ceramic particles within a polymer host, which resulted in uniform dispersion of the former in the latter and enhanced product properties.

The concept of preparing in situ formed polymer–ceramic composites is further expanded in this study. A novel approach is used to prepare a fully amorphous PEO–SiO_2 composite polymer electrolyte through simultaneous formation of the polymer matrix and the inorganic particles. Sol–gel transformation based on the hydrolysis and condensation of tetraethoxysilane (TEOS) is used to prepare the inorganic phase, concurrent with ultraviolet (UV) irradiation of poly(ethylene glycol) dimethacrylate (PEGDMA) and methoxy poly(ethylene glycol) monomethacrylate (PEGMA) to produce the PEO network. The morphology and the crystallinity of the composite are examined by transmission electron microscopy (TEM) and differential scanning calorimetry (DSC), respectively. Electrochemical properties of interest to battery applications, such as ionic conductivity and Li^+ transference number, are measured by electrochemical impedance spectroscopy (EIS).

2. Experimental

2.1. Materials

Macro-monomers with a PEO-like structure, PEGDMA with a molecular weight of 550, and PEGMA with a molecular weight of 300, were supplied by Aldrich (Milkaukee, MI, USA) and were used as polymer network precursors. The chemical structures of PEGDMA and PEGMA, with average EO units of 9 ($\overline{M}$ = 550) and 4.5 ($\overline{M}$ = 298), respectively, are as follows:

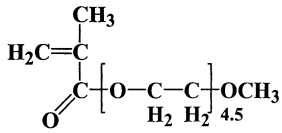

PEGMA

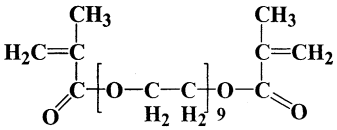

PEGDMA

2,2-Dimethoxy-2-phenyl-acetonphenone (DMPA), used as photoinitiator, and battery-grade lithium tetrafluoroborate ($LiBF_4$) were also purchased from Aldrich, as well as high surface area SiO_2 (255 $m^2\,g^{-1}$, particle size = 11 nm). Tetraethoxysilane (TEOS), used as precursor for the inorganic filler, was obtained from Fluka Chemie GmbH. Thirty-seven percent hydrochloric acid (catalyst) and dichloromethane (extraction solvent) were obtained from Merck (Darmstadt, Germany).

2.2. Preparation of composite polymer electrolytes

All procedures, unless otherwise specified, were carried out inside a Braun glove box with re-circulating argon to keep the moisture content below 1 ppm. About 2.5 g of polymer precursors with different PEGDMA to PEGMA ratios were mixed in a sample vial. Appropriate amounts of DMPA and $LiBF_4$ were then added. In all samples, DMPA was loaded at 1 wt.% with respect to the polymer precursors; $LiBF_4$ was introduced to give a constant O:Li ratio of 20:1. The mixture was stirred for 3 h in the dark to produce a clear and viscous solution, and spread between two glass plates that were separated by a Teflon spacer used for gap control. Polymerization was initiated using an EF280c Spectroline Irradiance Lamp (Spectronics Corporation, New York) with two 8 W tubes producing UV radiation at 254 nm. The monomer mixture was placed at about 10 cm from the lamp and exposed to the UV irradiation for 15 min. In this way, strong and completely transparent electrolyte membranes with a thickness of 200–300 μm could be obtained and were easily detached from the glass plates.

To synthesize the composite polymer electrolytes, TEOS was first pre-hydrolyzed in air under ambient conditions [27]. 2.5 ml TEOS and 0.4 ml deionized water were mixed in a sample vial under continuous stirring. 0.04 ml 0.15N HCl was used to catalyze the hydrolysis. The solution was then sonicated for 15 min to facilitate the conversion of ethoxy ligands to Si–OH groups. The hydrolyzed silica precursor (a sol) was then transferred to the glove box. A measured amount of the silica sol, based on the complete conversion of TEOS to SiO_2, was added to the abovementioned PEGDMA–PEGMA–$LiBF_4$ solution. The hydrolysis

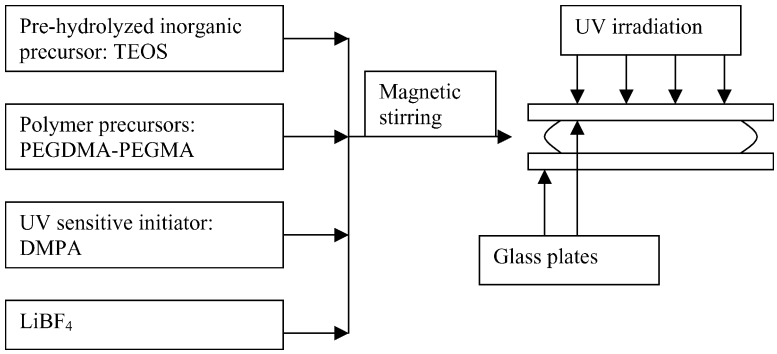

Fig. 1. Schematic representation of process of simultaneous formation of polymer network and inorganic nanoparticles.

and condensation reactions of TEOS can be summarily written as:

$$Si(OC_2H_5)_4 + 4H_2O \rightarrow Si(OH)_4 + 4C_2H_5OH \text{ (hydrolysis)}$$

$$nSi(OH)_4 \rightarrow SiO_2 + 2nH_2O \text{ (condensation)}$$

The polymer precursor–sol mixture was stirred vigorously for another 3 h at room temperature in the dark. The mixture was subsequently subjected to UV irradiation to form a composite matrix. For comparative purposes, PEO–SiO_2 composites were also prepared by the direct addition of Aldrich's SiO_2 nanoparticles to the polymer precursor solutions; while keeping the other steps in the preparation unchanged. This new process of the preparing PEO–SiO_2 composite electrolytes is shown schematically in Fig. 1.

2.3. Conversion of macromers to polymer network and DSC measurements

The conversion in the polymerization reaction was determined as follows. The irradiated nanocomposite sample was weighed (W_1) and then extracted with dichloromethane in a Soxhlet apparatus for 24 h. After extraction, the sample was dried at 50 °C in a vacuum oven for 1 day and weighed again (W_2). The conversion was determined as $(W_2/W_1) \times 100\%$. The glass transition temperature, T_g, of the composite was determined by differential scanning calorimetry (DSC) using a Mettler-Toledo analyzer that consisted of a DSC 822e main unit and STARe software. About 10 mg of sample was sealed in a standard aluminum pan inside the glove box to prevent exposure of the sample to moisture. The sample pan was then heated in nitrogen from −100 to 100 °C at the rate of 10 °C min^{-1}.

2.4. TEM measurements

A JEOL TEM-2010 microscope operating at 200 kV was used to image the inorganic particles in the composite polymer electrolytes. To this end, samples of the composite polymer electrolyte were heated at 650 °C for 6 h to decompose the organic components, while leaving the inorganic structure practically intact [28,29]. The solid residue was ball-milled, suspended in acetone, and sonicated. A drop of the suspension was placed on a 200-mesh copper grid covered with carbon film, and dried under ambient conditions prior to TEM examination.

2.5. Measurements of ionic conductivities and transference numbers

A sample membrane disc was sandwiched between two stainless-steel electrodes and assembled in a tightly sealed test cell. The cell was thermostatted and the temperature was varied between 30 and 70 °C. The electrochemical impedance of the cell was measured between 1 Hz and 1 MHz using an Eco Chemie PGSTAT 30 potentiostat/galvanostat equipped with a frequency response analyzer module. Ionic conductivity was calculated from the impedance response according to established procedures [30]. For measurements of Li^+ transference numbers, lithium metal was used as both electrodes to constitute a symmetric test cell with the structure: Li|composite polymer electrolyte|Li. The assembled cell was thermostatted at 70±1 °C. A first measurement of electrochemical impedance was taken before a dc bias of 10 mV was applied to the cell. The current response of the cell was monitored until a steady-state was reached. Another measurement of the cell impedance was then made to complete the procedure.

3. Results and discussion

3.1. Morphology of PEO–SiO_2 organic–inorganic hybrid

A TEM image of the calcined PEO–SiO_2 composite from PEGDMA and 5 wt.% of in situ formed SiO_2 is shown in Fig. 2. Small SiO_2 particles of about 10–20 nm in diameter and with a narrow size distribution are found. The nanoparticles are dispersed well within the remains of the polymer matrix, and show no sign of extensive particle agglomeration even after thermal treatment. The present method of preparation is therefore able to produce and maintain a high dispersion of the inorganic phase in the polymer matrix.

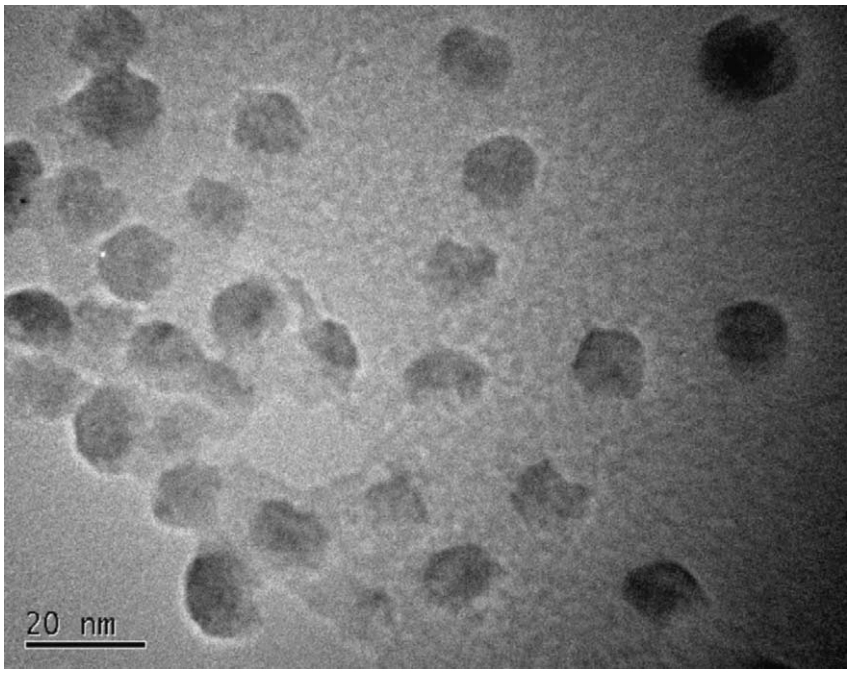

Fig. 2. Typical TEM image of composite electrolyte from calcined sample (for PEGDMA and 5 wt.% of in situ formed SiO_2).

In the present method of preparation, TEOS is converted into SiO_2 via a sol–gel process that takes place within a growing polymer network. The mobility of the hydrolyzed precursor molecules is substantially reduced by the viscous PEGDMA macro-monomer and steric hindrance. As a result, the probability of the resulting sol nuclei meeting one another to grow into an extended structure or large particles is greatly reduced. The mobility of the growing SiO_2 particles is further reduced after the reaction medium is irradiated with UV light. The rapid polymerization of PEGDMA into a PEO-like network significantly and quickly increases the viscosity of the reaction medium, and locks the liquid-phase homogeneity into the final solidified product. Under such conditions, only a limited amount of sol particles are able to undergo gelation to form large assemblies, and most SiO_2 exists as isolated nanoscale particles which are uniformly dispersed in the polymer network.

3.2. Structure of cross-linked polymer

The UV irradiation of PEGDMA macro-monomer results in an extremely brittle membrane, which limits its practicality as a polymer electrolyte or battery separator—a glassy polymer would have difficulty in keeping its dimensional integrity under external pressure or tensile elongation when used in the battery fabrication process [31]. Hence, a second macro-monomer, PEGMA, has been introduced to adjust the softness of the electrolyte membrane. The mechanical properties of the electrolyte membranes with different PEGMA contents are summarized qualitatively in Table 1.

The addition of PEGMA, a macro-monomer with a single functional group, can increase significantly the flexibility of the electrolyte membranes as shown in Table 1. The polymer becomes flexible when the degree of cross-linking is reduced to 45%. The enhanced flexibility is due to increased separation between adjacent network junction points. This

Table 1
Conversion, T_g and mechanical properties of cross-linked polymers

PEGMA (%)	PEGDMA (%)	Conversion (%)	Theoretical cross-linking degree (%)[a]	T_g (°C)	Mechanical property[b]
0	100	98.4	100	−1.2	Brittle
30	70	97.9	56.1	−11.9	Brittle
40	60	97.2	44.9	−13.0	Flexible
50	50	96.6	35.1	−14.9	Flexible
60	40	95.9	26.5	−20.0	Flexible
70	30	95.2	18.8	−21.7	Flexible
80	20	93.6	11.9	−23.4	Flexible and weak

[a] Calculated by: $n_{PEGDMA}/(n_{PEGMA} + n_{PEGDMA})$.
[b] From manual bending test.

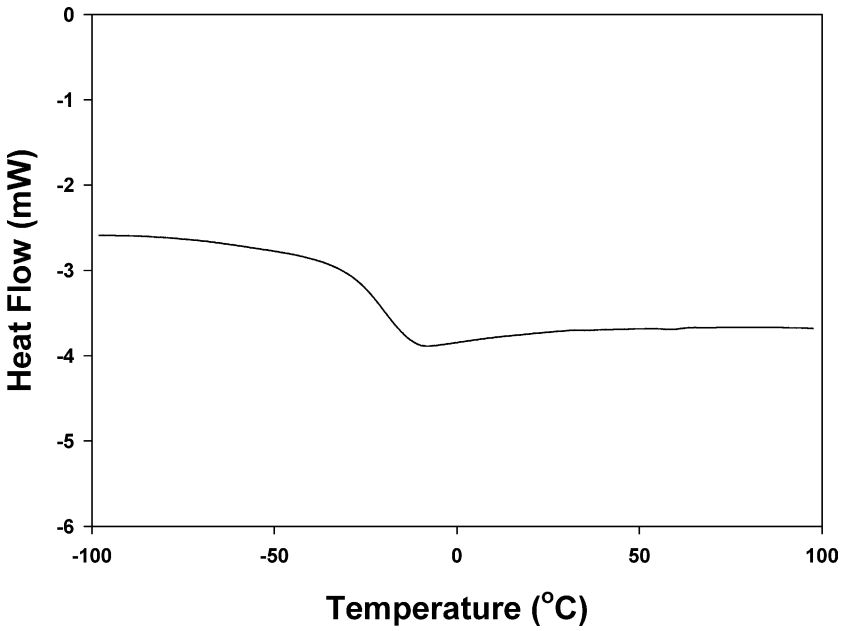

Fig. 3. Typical DSC response of cross-linked polymer electrolyte (for PEGDMA–PEGMA ratio of 30:70).

is confirmed by the change in T_g shown in Table 1. It should also be noted that too low a degree of cross-linking would not form freestanding films.

A typical DSC response of the cross-linked polymer (for a PEGDMA–PEGMA ratio of 30:70) is shown in Fig. 3. There is no fusion peak present in the temperature range −100 to 100 °C. This contrasts strongly with conventional PEO-based electrolytes which normally display an endothermic melting peak at around 60 °C [32]. The absence of a melting peak is taken as evidence of a fully amorphous structure in the PEO-like cross-linked network, which is established by the formation of a brush-like chain structure from polymerization of the PEGMA. The cross-linked structure also prevents the PEO segments from freely packing into a long-range ordered crystalline structure. The degree of cross-linking is, however, sufficiently moderated to allow short-range segmental movement to support uninhibited ion conduction. The apparent curvature in the DSC trace at sub-ambient temperatures is the glass transition range.

Since the glass transition temperature (T_g) of a polymer is closely related to the flexibility of the polymer chains, the cross-linking density is a determining factor in the measured T_g values. It is expected that the greater flexibility associated with a low cross-linking density should lead to a low T_g [33], despite the need for a certain amount of cross-linking to suppress the ordered folding of PEG chains. The T_g values in Table 1 illustrate such a trend. Since ion conduction in a polymer electrolyte is mostly due to the movement of the polymer chains, a low T_g is considered beneficial to ion conduction. The data in the following section will show that ionic conductivity is indeed higher in systems with lower cross-linking densities, i.e., a higher PEGMA content.

After taking into consideration the relative importance of the mechanical properties and ionic conductivity, a PEGDMA–PEGMA ratio of 30:70 was chosen as an exploratory polymer composition to formulate the polymer–ceramic composite system. Some of the measured properties of the polymer composites used in this study are shown in Table 2.

It is found that the addition of both Aldrich SiO_2 and in situ formed SiO_2 causes a decrease in T_g. This observation can be rationalized in terms of hydrogen bonding between the surface OH groups of SiO_2 nanoparticles and the ether oxygen atoms on the PEG branches (Fig. 4). This will skew the polymer chains and result in additional free volume. It appears that this irregular chain-folding effect perturbs the bulk of polymer phase and causes causing a reduction in the matrix density and hence a higher local mobility for the polymer segments. A weakened O:Li complexation, resulting from the competitive hydrogen bonding, could also contribute to the increased segmental motion. By contrast, the segment motion of those polymer chains in contact with the SiO_2 particles might become more restrained by the same hydrogen bonding. Special attention should be paid to the sample with in situ formed SiO_2 because a relatively large

Table 2
T_g and mechanical properties of polymer composite membranes

Sample	T_g (°C)	Mechanical properties
PEGDMA–PEGMA (30:70)	−21.7	Flexible
PEGDMA–PEGMA–SiO_2–5%-m[a]	−21.9	Flexible
PEGDMA–PEGMA–SiO_2–5%-h[b]	−23.9	Flexible

[a] Mechanical blending with Aldrich SiO_2.
[b] With in situ formed SiO_2.

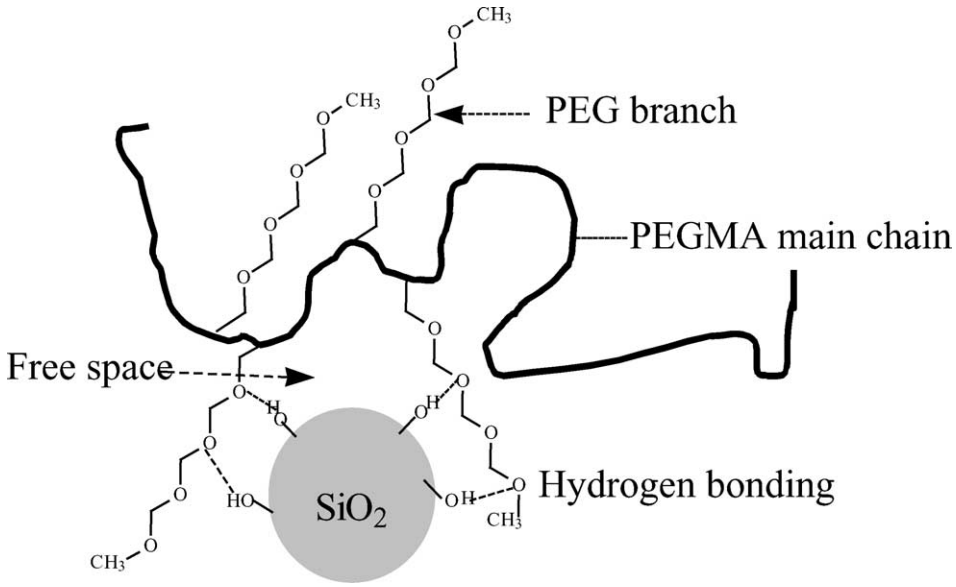

Fig. 4. Schematic representation of interaction between polymer chains and surface groups of SiO_2 particles.

change in T_g is observed, and suggests a greater extent of hydrogen bonding because more surface OH– groups are available from SiO_2 prepared by the sol–gel process. This is not unexpected if the SiO_2 particles are formed through the condensation of only a finite number of $Si(OH)_4$ units (hydrolytic product of TEOS).

3.3. Electrochemical properties of the composite polymer electrolytes

For conductivity measurements using two blocking electrodes to sandwich the polymer electrolyte, the following equation may be used:

$$\sigma = \frac{d}{R_b r^2 \pi} \quad (1)$$

where d and r represent the thickness and the radius of the sample membrane discs, respectively. R_b is the bulk resistance of the nanocomposite electrolyte from complex impedance measurements. It is commonly accepted that R_b can be obtained from the real-axis intercept at the high frequency end of the NyQuist plot of complex impedance [30,34].

As mentioned earlier, ion conduction in polymer electrolytes is coupled to the segmental motion of the polymer

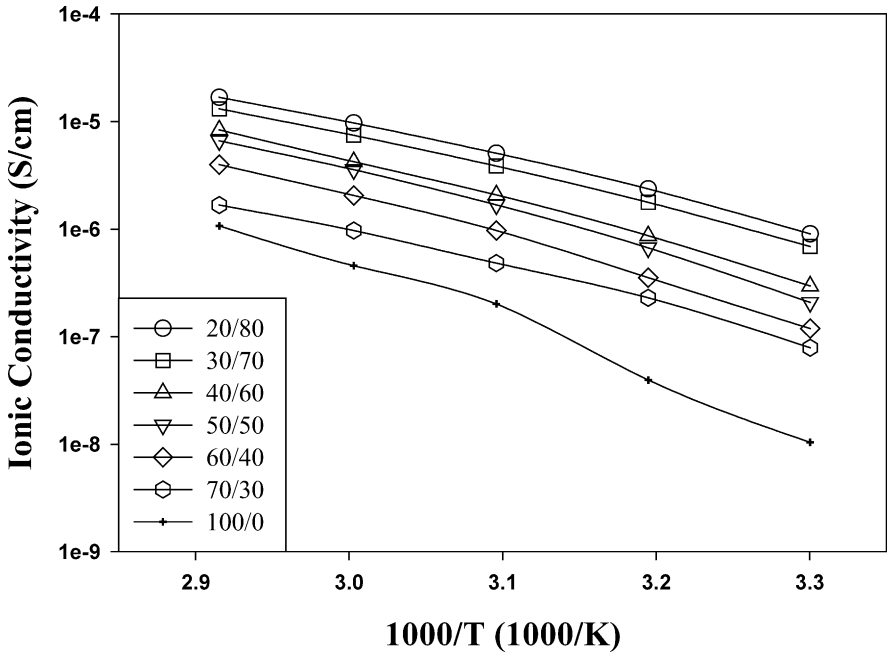

Fig. 5. Temperature dependence of ionic conductivity of cross-linked polymer electrolytes at different PEGDMA–PEGMA ratios.

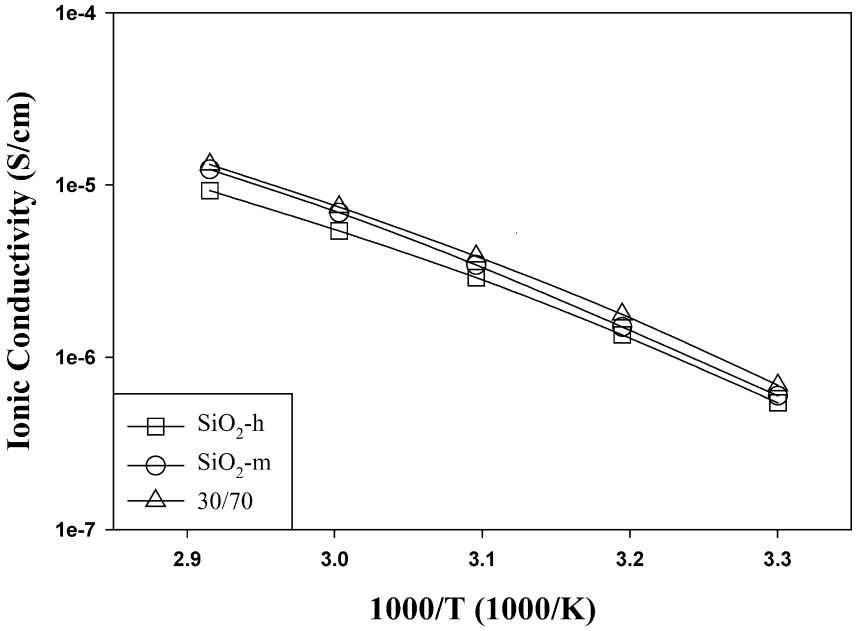

Fig. 6. Temperature dependence of ionic conductivity of cross-linked composite polymer electrolytes with in situ formed and Aldrich SiO_2.

chains. Hence ionic conductivity is affected by the cross-linking density and the value of T_g. The temperature dependence of ionic conductivity of cross-linked polymer electrolytes at different PEGDMA–PEGMA ratios is shown in Fig. 5. The trend is a general increase in ionic conductivity with the PEGMA content. The lower T_g in electrolytes with higher PEGMA contents is largely responsible for the increase in conductivity. This trend is not, however, observed in polymer composite electrolytes that contain SiO_2, as shown in Fig. 6. Although T_g is lowered after the addition of either Aldrich or in situ formed SiO_2, the ionic conductivity actually decreases (slightly) instead of increasing. This is probably due to interactions between the surface hydroxyl groups and anions, BF_4^- in this case, to form hydrogen bonds of the type F∼H–O; although these bonds are relatively weak compared with normal hydrogen bonds. Furthermore, additional free space is created near the particle surface after SiO_2 addition, as shown in Fig. 4. Such free volume could favour an adsorption-like process, in which the mobility of the larger BF_4^- anions is hindered near the SiO_2 surface through multiple hydrogen bondings. The extent of these effects is expected to depend on the concentration of the surface OH groups. Since the surface OH concentration is higher in in situ formed SiO_2, the anion mobility in the in situ formed composite was further reduced compared with the composite formulated with Aldrich SiO_2. A lower overall conductivity is therefore observed in this case.

Measurements of Li^+ transference numbers of the polymer composite electrolytes provide additional evidence on the different changes to the cation and anion mobilities in the polymer. The transference numbers are determined by the method of Evans et al. [35]. In this method, a test cell with the symmetric Li|composite electrolyte|Li configuration is used. A typical current transient from such a test cell under a constant small dc voltage perturbation is shown in Fig. 7. After taking into consideration the growth in passivation layer and the establishment of concentration gradient, the Li^+ transference number in the electrolyte can be calculated as [35]:

$$T_+ = \frac{I_s(\Delta V - I_0 R_0)}{I_0(\Delta V - I_s R_s)} \quad (2)$$

where ΔV is the value of the applied dc bias (10 mV), R_0 and R_s the initial and final (steady-state) resistances of the passivation layer, which can be obtained through complex impedance measurements; I_0 and I_s are the initial and steady-state currents. The resulting transference numbers are summarized in Table 3:

The Li^+ transference number for the cross-linked polymer electrolytes without SiO_2 is 0.29, a value which is fairly close to the higher end of most PEO-based polymer electrolytes ($t_{Li} = 0.1$–0.3). This implies a conduction mechanism that depends mostly on polymer chain movement. The addition of Aldrich SiO_2 increases the Li transference number slightly (0.34), which indicates that some, but limited interactions between Aldrich SiO_2 particles, cations, anions, and the ether oxygen atoms to give rise to an increase in Li^+ mobility and a decrease in BF_4^- mobility. Finally, for

Table 3
Transference numbers of composite polymer electrolytes

Sample	Transference number
PEGDMA–PEGMA (30:70)	0.29
PEGDMA–PEGMA–SiO_2–5%-m	0.34
PEGDMA–PEGMA–SiO_2–5%-h	0.56

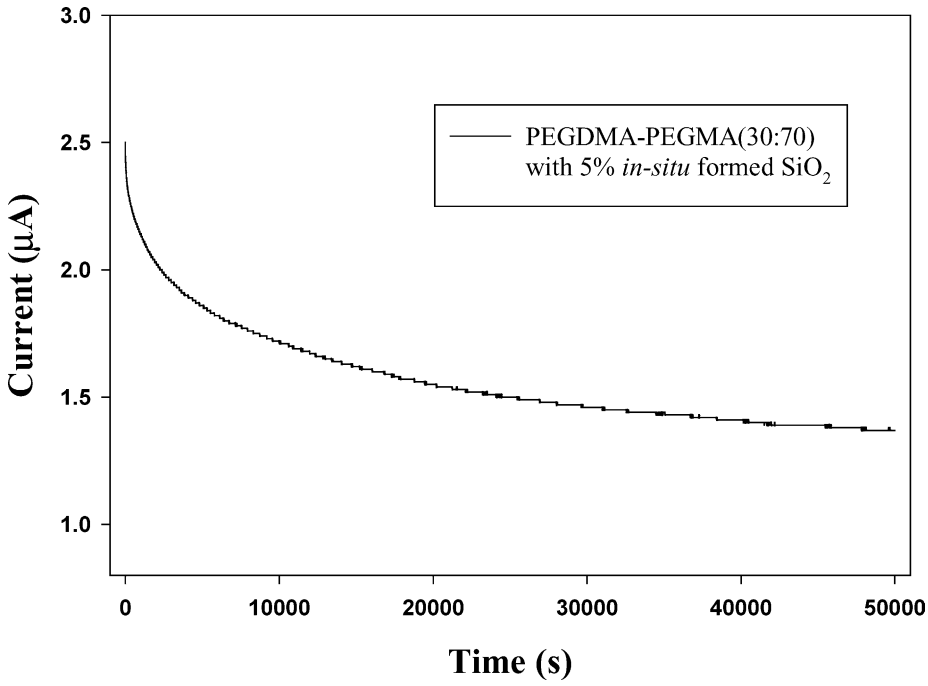

Fig. 7. Current response of a Li/amorphous PEO–SiO_2 composite electrolyte|Li assembly under dc voltage (10 mV) as function of time.

the composite electrolyte containing in situ formed SiO_2, the Li transference number increases substantially to 0.56. The much stronger interactions (arising from a higher concentration of surface OH groups per unit volume) between the in situ formed SiO_2 nanoparticles, anions, cations, and the polymer chains are again implicated by this experimental observation.

4. Conclusions

Previous work has shown that the use of SiO_2 fillers in PEO-based composite electrolytes improves ionic conductivity. At first, this was attributed to suppression of PEO crystallization in the presence of the inorganic particles. Recently, chemical interactions between ceramic particles, Li salt and the polymer are also believed to contribute to the conductivity enhancement. In this investigation, fully amorphous nanocomposite polymer electrolytes are made and allow the investigation of chemical interactions between the various electrolyte components without the added complexity of the crystallinity effect.

UV irradiation is used to initiate the polymerization of PEGDMA–PEGMA macro-monomers into completely amorphous polymer electrolytes. DSC measurements have confirmed the amorphicity, and the T_g value of the electrolytes is related to the cross-linking density of the polymer network. The single functionality macro-monomer PEGMA is used to adjust the cross-linking density of the system. A lower T_g and an improved conductivity are obtained from electrolytes containing a higher PEGMA content.

A sol–gel process is used for the in situ formation of the SiO_2 particles. The chemical polymerization of the silica sol and the UV polymerization of the macro-monomers ae carried out concurrently to enable the simultaneous formation of the polymer network and the inorganic nanoparticles. Electrochemical measurements show slightly lower ionic conductivity, but substantially higher transference number, when the in situ formed SiO_2 is used. This is interpreted in terms of chemical interactions between the OH groups on the ceramic particles, the cations and anions, and the ether oxygen atoms on the polymer backbone. The interactions are believed to result in the increase in Li mobility and the decrease in the anion mobility.

To date, it has not been possible to provide direct evidence of the interactions between the inorganic nanoparticles, the cations and anions, and the ether oxygen atoms on the polymer backbone. There are plans to use FTIR, NMR and other molecular spectroscopic techniques in future work to probe the changes in the local environment of the different atoms.

References

[1] J.R. MacCallum, C.A. Vincent, Polymer Electrolyte Reviews, vol. I, Elsevier, London, 1987.
[2] J.R. MacCallum, C.A. Vincent, Polymer Electrolyte Reviews, vol. II, Elsevier, London, 1989.
[3] M. Armand, Solid State Ionics 9 (1983) 745.
[4] M. Armand, J.M. Chabagno, M. Duclot, Fast Ion Transport in Solids, North-Holland, Amsterdam, 1979, p. 131.
[5] C. Bertier, W. Gorecki, M. Mimier, M.B. Armand, J.M. Chabagno, P. Rigaud, Solid State Ionics 11 (1983) 91.

[6] A. Bouridah, F. Dalard, D. Deroo, H. Cheradame, J.F. Le Nest, Solid State Ionics 15 (1985) 233.
[7] P.M. Blonsky, D.F. Shriver, P. Austin, H.R. Allcock, J. Am. Chem. Soc. 106 (22) (1984) 6854.
[8] E. Tsuchida, H. Ohno, K. Tsunemi, Electrochim. Acta 28 (1983) 591.
[9] J.M. Tarascon, A.S. Gozdz, C. Schmutz, F. Shokoohi, P.C. Warren, Solid State Ionics 86–88 (1996) 49.
[10] J.E. Weston, B.C.H. Steele, Solid State Ionics 7 (1982) 75.
[11] W. Wieczorek, K. Such, H. Wycislik, J. Plocharski, Solid State Ionics 36 (1989) 255.
[12] F. Capuano, F. Croce, B. Scrosati, J. Electrochem. Soc. 138 (1991) 1918.
[13] A. Chandra, P.C. Srivastava, C. Chandra, J. Mater. Sci. 30 (1995) 3633.
[14] B. Kumar, S.J. Rodrigues, J. Electrochem. Soc. 148 (2001) A1336.
[15] W. Krawiec, L.G. Scanlon, J.P. Fellner, R.A. Vaia, S. Vasudevan, E.P. Giannelis, J. Power Sources 54 (1995) 310.
[16] C. Capiglia, P. Mustarelli, E. Quartarone, C. Tomasi, A. Magistris, Solid State Ionics 118 (1999) 73.
[17] J. Fan, S.R. Rafhavan, X.Y. Yu, S.A. Khan, P.S. Fedkiw, J. Hou, G.L. Baker, Solid State Ionics 111 (1998) 117.
[18] S.H. Chung, Y. Wang, L. Persi, F. Croce, S.G. Greenbaum, B. Scrosati, E. Plichta, J. Power Sources 97–98 (2001) 644.
[19] F. Croce, G.B. Appetecchi, L. Persi, B. Scrosati, Nature 456 (1998).
[20] M. Forsyth, D.R. MacFarlane, A. Best, J. Adebahr, P. Jacobsson, A.J. Hill, Solid State Ionics 147 (2002) 203.
[21] A.S. Best, J. Adebahr, P. Jacobsson, D.R. MacFarlane, M. Forsyth, Macromolecules 34 (2001) 4549.
[22] A.S. Best, A. Ferry, D.R. MacFarlane, M. Forsyth, Solid State Ionics 126 (1999) 269.
[23] H.J. Walls, J. Zhou, J.A. Yerian, P.S. Fedkiw, S.A. Khan, M.K. Stowe, G.L. Baker, J. Power Sources 89 (2000) 156.
[24] J.O. Kweon, S.T. Noh, J. Appl. Polym. Sci. 81 (2001) 2471.
[25] N.C. Mello, T.J. Bonagamba, H. Panepucci, K. Dahmouche, P. Judeinstein, M.A. Aegerter, Macromolecules 33 (2000) 1280.
[26] P.H. de Souza, R.F. Bianchi, K. Dahmouche, P. Judeinstein, R.M. Faria, T.J. Bonagamba, Chem. Mater. 13 (2001) 3685.
[27] P.W. Wu, S.R. Holm, A.T. Duong, B. Dunn, R.B. Kaner, Chem. Mater. 9 (1997) 1004.
[28] L.M. Bronstein, C. Joo, R. Karlinsey, A. Ryder, J.W. Zwanziger, Chem. Mater. 13 (2001) 3678.
[29] C.G. Goltner, S. Henke, M.C. Weissenberger, M. Antonietti, Angew. Chem. Int. Ed. 37 (1998) 613.
[30] M. Watanabe, K. Sanui, N. Ogata, T. Kobayashi, Z. Ohtaki, J. Appl. Phys. 57 (1985) 123.
[31] K.H. Lee, K.H. Kim, H.S. Lim, J. Electrochem. Soc. 148 (2001) A1148.
[32] B. Kumar, L. Scanlon, R. Marsh, R. Mason, R. Higgins, R. Baldwin, Electrochim. Acta 46 (2001) 1515.
[33] A. Eisenberg, Physical Properties of Polymers, Second ed., American Chemical Society, Washington, 1993, p. 88.
[34] K.M. Abraham, Z. Jiang, B. Carroll, Chem. Mater. 9 (1997) 1978.
[35] J. Evans, C.A. Vincent, P.G. Bruce, Polymer 28 (1987) 2324.